

## SUPPORTING INFORMATION

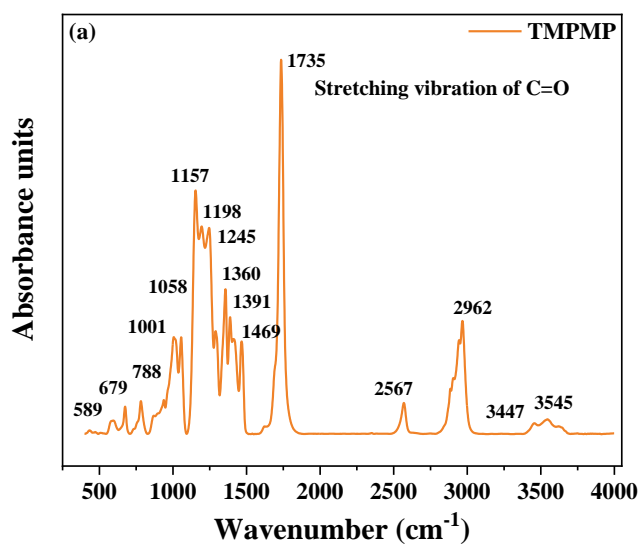
### Enhanced Interfacial Compatibility and Dynamic Fatigue Crack Propagation Behavior of Natural Rubber/Silicone Rubber Composites

*Qingyuan Han*<sup>†</sup>, *Liqun Zhang*<sup>†,‡</sup>, *Youping Wu*<sup>\*,†,‡</sup>

<sup>†</sup>State Key Lab of Organic-Inorganic Composites, Beijing University of Chemical Technology, Beijing 100029, PR China

<sup>‡</sup>Beijing Engineering Research Center of Advanced Elastomers, Beijing University of Chemical Technology, Beijing 100029, PR China

The FT-IR spectrums of TMPMP; pure NR (T0-D0) and extracted T-NRs (T0.5-D0.05, T1-D0.1, T1.5-D0.15) are shown in **Figure S1 (a)** and **(b)**, respectively.



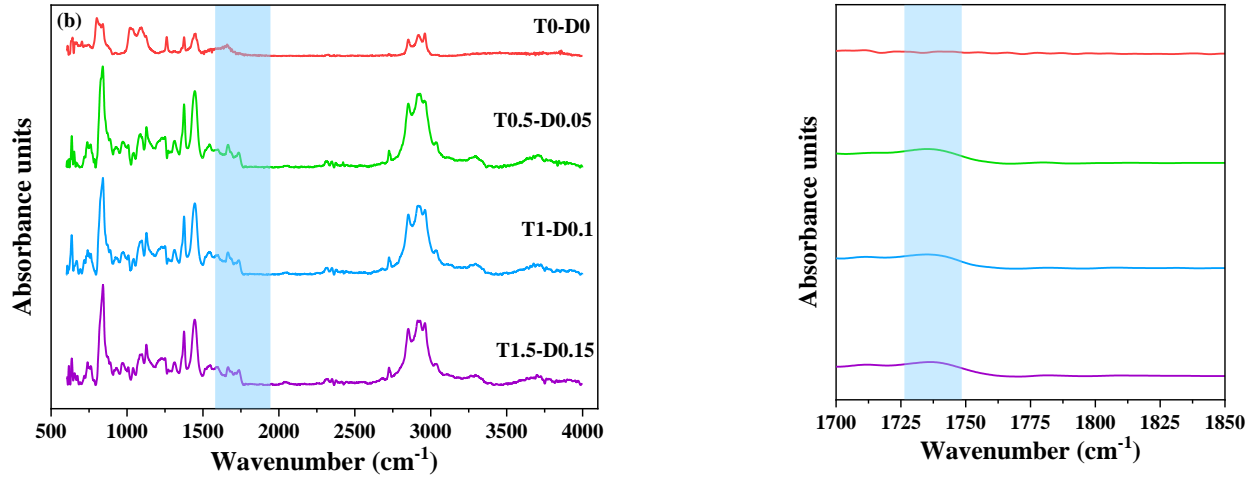


**Figure S1.** FT-IR spectrums of (a) TMPMP; (b) pure NR (T0-D0) and extracted T-NRs (T0.5-D0.05, T1-D0.1, T1.5-D0.15), including enlarged details

Comparing with pure NR (T0-D0), the stretching vibration peaks of carbonyl groups (C=O) in TMPMP around  $1735\text{ cm}^{-1}$  (**Figure S1 (a)**) have been retained in the extracted T-NRs (enlarged details in **Figure S1 (b)**), which proves the successful grafting of TMPMP on NR.

The interfacial adhesive energy ( $W_{\text{rf}}$ ) between rubber and filler could be calculated by Fowkes model [26], which is an effective criterion for evaluating the interfacial interaction degree between rubber and filler:

$$W_{\text{rf}} = 2(\sqrt{\gamma_r^d \gamma_f^d} + \sqrt{\gamma_r^p \gamma_f^p}) \quad (\text{S1})$$

where  $\gamma_r^d$  and  $\gamma_r^p$  are dispersive and polar part of surface energy for rubber, respectively, and  $\gamma_f^d$  and  $\gamma_f^p$  are dispersive and polar part of surface energy for filler, respectively. The surface energy ( $\gamma$ ) and its dispersive/polar part ( $\gamma_D/\gamma_P$ ) for NR and VMQ were measured in our earlier study [9], and the surface energy of silica has referred to the result of Heinrich et al [27], for the same brand VN3 used, then the  $W_{\text{rf}}$  was determined as listed in **Table S1**. The higher  $W_{\text{rf}}$  of NR-silica than that of VMQ-silica indicates the stronger interfacial interaction between NR phases and silica.

In addition, according to **Equation (S2)**, the interfacial energy ( $\gamma_{12}$ ) between any two components is correlated to their surface energy  $\gamma_1$  and  $\gamma_2$ , then the phase selective distribution of silica could be further assessed by the wetting coefficient ( $\omega_{\text{NR-VMQ}}$ ) [28], which is a function of interfacial energy among silica, NR and VMQ:  $\gamma_{\text{silica-NR}}$ ,  $\gamma_{\text{silica-VMQ}}$  and  $\gamma_{\text{NR-VMQ}}$ . As for  $\omega_{\text{NR-VMQ}} > 1$ , silica would distribute in NR phases; with regard to  $\omega_{\text{NR-VMQ}} < -1$ , silica would distribute in VMQ phases; when  $-1 < \omega_{\text{NR-VMQ}} < 1$ , silica would distribute at the interface of the two phases.

$$\gamma_{12} = \gamma_1 + \gamma_2 - 2(\gamma_1\gamma_2)^{\frac{1}{2}} \quad (\text{S2})$$

$$\omega_{\text{NR-VMQ}} = \frac{(\gamma_{\text{silica-VMQ}} - \gamma_{\text{silica-NR}})}{\gamma_{\text{NR-VMQ}}} \quad (\text{S3})$$

Corresponding interfacial energy and wetting coefficient have also been determined in **Table S1**.

As for  $\omega_{\text{NR-VMQ}} = 9 \gg 1$ , demonstrating the selective location tendency of silica in NR phases.

Therefore, these two parameters:  $W_{\text{rf}}$  and  $\omega_{\text{NR-VMQ}}$ , could both reasonably explain the reason why part of pre-mixed silica in VMQ/silica master-batch has migrated from VMQ phases internal into NR phases after compounding, as the result shown in **Figure 4**.

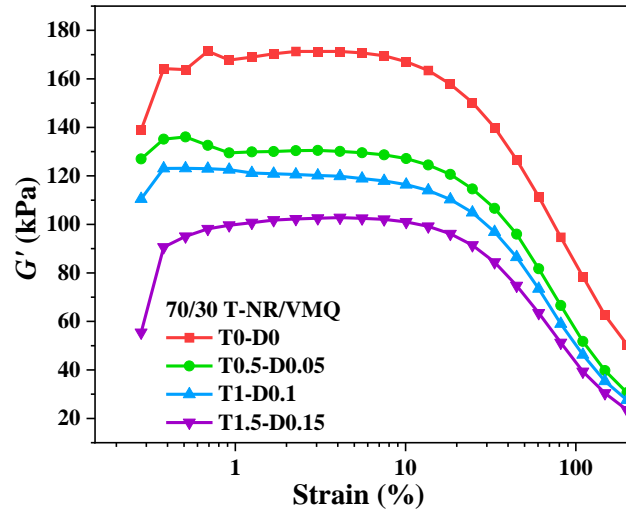
**Table S1.** Surface energy ( $\gamma$ ) and its dispersive/polar part ( $\gamma_{\text{D}}/\gamma_{\text{P}}$ ) for NR, VMQ and silica; interfacial adhesive energy ( $W_{\text{rf}}$ ), interfacial energy ( $\gamma_{12}$ ) among them (NR-silica, VMQ-silica, NR-VMQ) and wetting coefficient ( $\omega_{\text{NR-VMQ}}$ )

| Surface energy (mN/m) | Total $\gamma$ | Dispersive part ( $\gamma_{\text{D}}$ ) | Polar part ( $\gamma_{\text{P}}$ ) |
|-----------------------|----------------|---|------------------------------------|
| NR                    | 25.2           | 25.2                                    | 0                                  |
| VMQ                   | 23.0           | 23.0                                    | 0                                  |
| silica                | 34.9           | 19.7                                    | 15.2                               |

|                                       |                          |
|---------------------------------------|--------------------------|
| Interfacial adhesive energy<br>(mN/m) | $W_{\text{rf}}$          |
| NR-silica                             | 44.6                     |
| VMQ-silica                            | 42.6                     |
| Interfacial energy (mN/m)             | $\gamma_{12}$            |
| NR-silica                             | 0.79                     |
| VMQ-silica                            | 1.24                     |
| NR-VMQ                                | 0.05                     |
| Wetting coefficient                   | $\omega_{\text{NR-VMQ}}$ |
|                                       | 9                        |

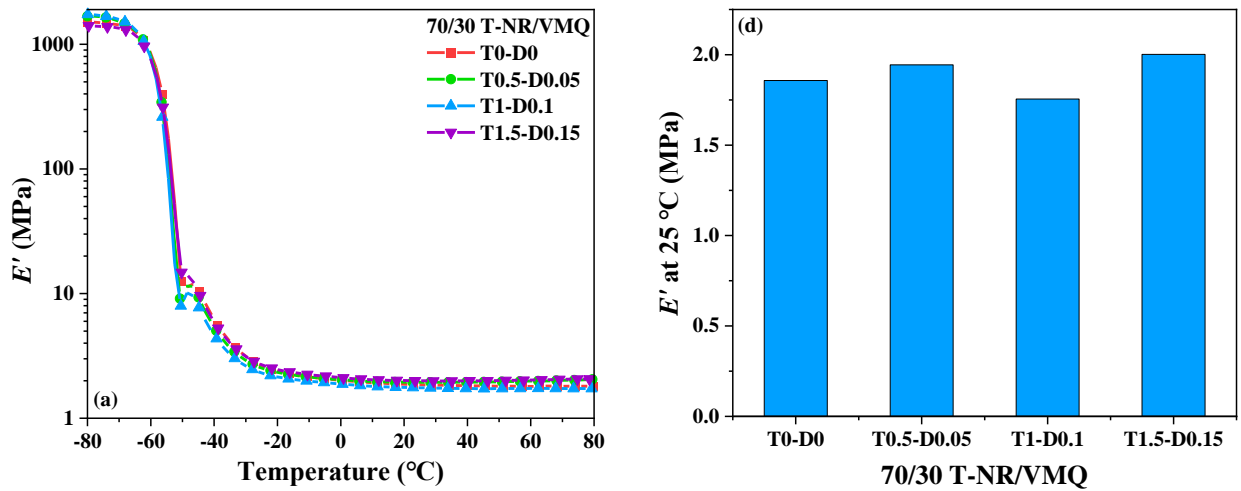
RPA was conducted to investigate the agglomeration degree of silica in composites, the storage modulus ( $G'$ )-strain sweeping curves of T-NR/VMQ composites are shown in **Figure S2**. The high  $G'$  level at lower strains and its rapid decrease at higher strains is called Payne effect [29], which is mainly caused by the existence of filler network under lower strains and its progressive collapse and destruction under higher strains. The more  $G'$  decrease amplitude ( $\Delta G'$ ), the stronger structure of filler network, the worse dispersion of filler in rubber matrix, the lower rubber-filler interaction. As could be seen, with the increase of TMPMP grafting degree, the  $\Delta G'$  gradually decreases, which indicates the weakened filler network, the explanations for this result are as below: as discussed above, due to the small amount of silica (10.5 phr) was pre-mixed in VMQ/silica master-batch, after compounding with NR, part of silica has migrated into the large amount of NR matrix (70 phr), which is helpful to weaken the packing of silica network; besides, under the

modification via TMPMP, the smaller sized and more evenly distributed VMQ phases in NR matrix is another assistance to facilitate a more homogeneous dispersion of silica in composites.



**Figure S2.** RPA storage modulus ( $G'$ )-strain sweeping curves of T-NR/VMQ composites

The temperature dependency of storage modulus ( $E'$ ), loss factor ( $\tan \delta$ ) and loss compliance modulus ( $J''$ ) measured via DMTA is shown in **Figure S3 (a)-(c)**, respectively, and the corresponding values at 25 °C (consistent with the testing temperature of dynamic fatigue crack growth) are listed in the histograms of **Figure S3 (d)-(f)**, respectively.



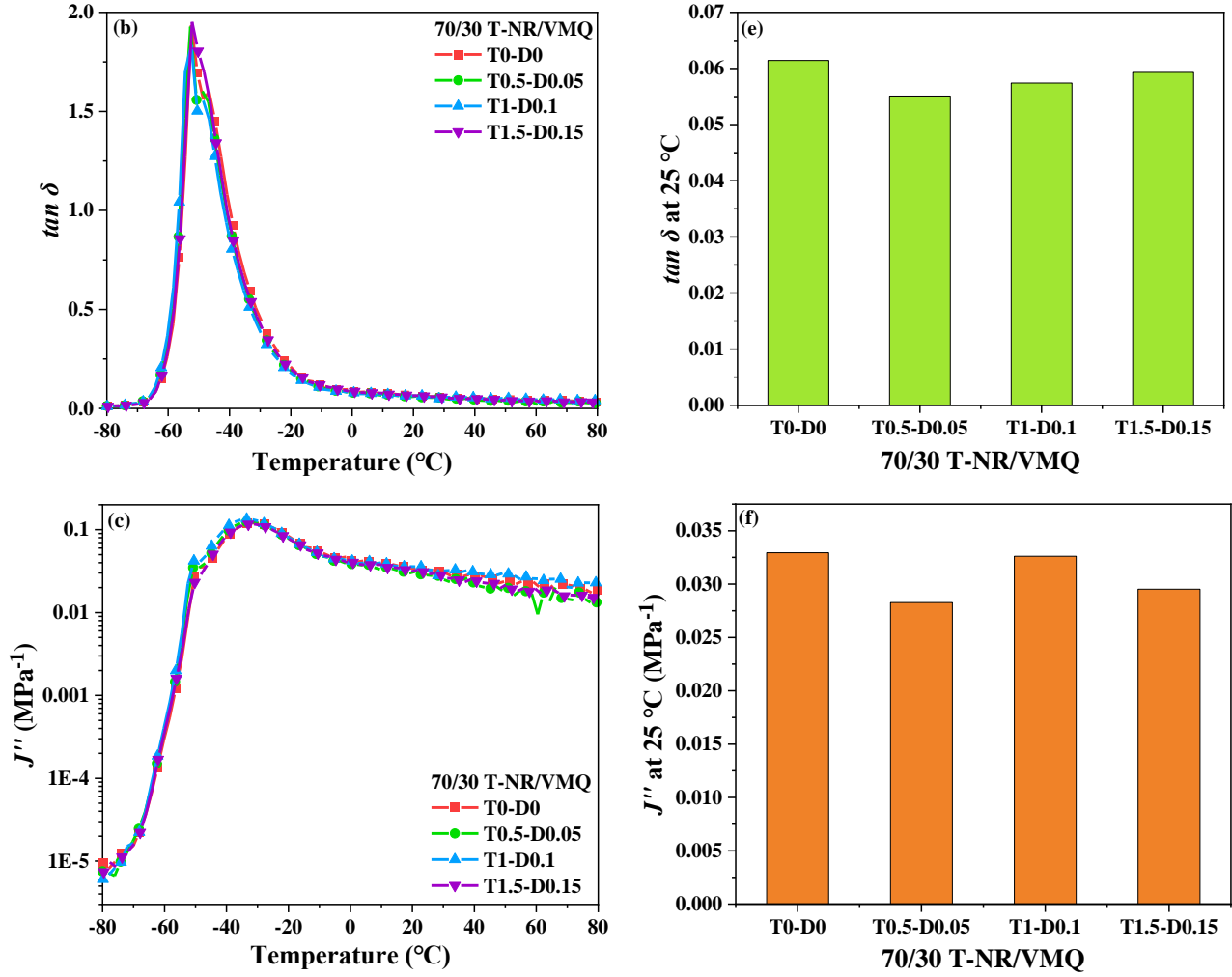


**Figure S3.** Temperature dependency of (a) storage modulus ( $E'$ ), (b) loss factor ( $\tan \delta$ ) and (c) loss compliance modulus ( $J''$ ); (d)-(f): corresponding values at 25 °C for T-NR/VMQ composites via DMTA

The cyclic stress-strain curves recorded in the real-time during crack growth are shown in **Figure S4**, as for the strain amplitude is about 20 %, the composites exhibit approximately a linear stress-strain behavior, which is consistent with the hypothesis of **Equation (3)** for Persson's theory.

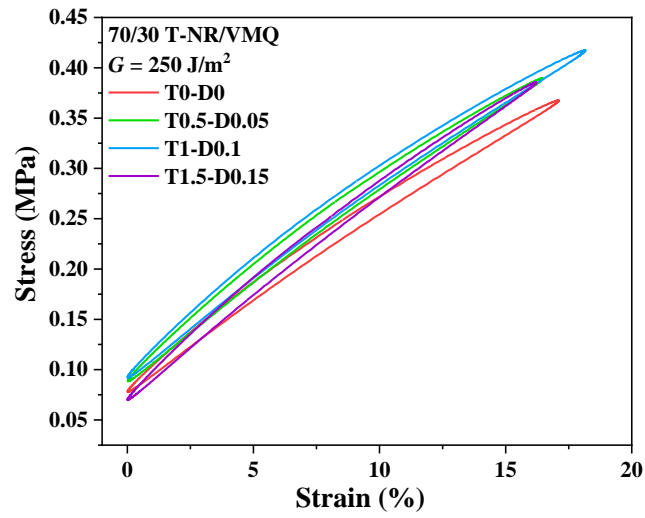


**Figure S4.** The cyclic stress-strain curves during crack growth for T-NR/VMQ composites